Received: 14 July 2021 | Revised: 1 October 2021 | Accepted: 3 April 2022

DOI: 10.1111/ejss.13239

ORIGINAL ARTICLE

European Journal of Soil Science WILEY

Fairy ring-induced soil potassium depletion gradients reshape microbial community composition in a montane grassland

Antonio Rodríguez[1,2] | **Mercedes Ibáñez**[1,2] | **Roland Bol**[3] | **Nicolas Brüggemann**[3] | **Agustín Lobo**[4] | **Juan José Jimenez**[5] | **Liliane Ruess**[6] | **M.-Teresa Sebastià**[1,2]

[1]Group GAMES, Department of Horticulture, Botany and Landscaping, School of Agrifood and Forestry Science and Engineering, University of Lleida, Lleida, Spain

[2]Laboratory of Functional Ecology and Global Change (ECOFUN), Forest Science and Technology Centre of Catalonia (CTFC), Solsona, Spain

[3]Institute of Bio- and Geosciences, Agrosphere (IBG-3), Jülich, Germany

[4]Institute of Earth Sciences "Jaume Almera" (CSIC), Barcelona, Spain

[5]Pyrenean Institute of Ecology (IPE-CSIC), Jaca, Huesca, Spain

[6]Institute of Biology, Ecology Group, Humboldt-Universität zu Berlin, Berlin, Germany

Correspondence
Antonio Rodríguez, Group GAMES, Department of Horticulture, Botany and Landscaping, School of Agrifood and Forestry Science and Engineering, University of Lleida, Alcalde Rovira-Roure Street, 191, Lleida 25198, Spain.
Email: antoniorodriguez@hbj.udl.cat

Funding information
COST Action ES1406; Universitat de Lleida; Spanish Science Foundation FECYT- MINECO, Grant/Award Numbers: IMAGINE, BIOGEI, CGL2017-85490-R, GL2013-49142-C2-1-R

Abstract

Fairy rings promoting circular greening belts in the vegetation can shape soil microbial communities by altering soil conditions. Knowledge about soil variables involved in this process is incomplete. We characterised the soil microbial communities of six fairy rings in a montane grassland using phospholipid fatty acid (PLFA) profiling, and studied if changes in soil properties corresponded to changes in soil microbial PLFA patterns. Exchangeable potassium (K) decreased inside the current rings, while soil moisture increased in the zones where the greening belts were two years before sampling (R2015). Fairy ring associated changes in PLFA composition were highly related to soil K. Gram-negative bacteria were associated with the zones outside the ring with the highest K content, whereas Gram-positive bacteria proportions increased inside the ring-affected zones. An environmental stress indicator, the *iso* to *anteiso* ratio of PLFA 17:0, decreased in the R2015 zones, coinciding with the highest soil moisture contents. Our findings highlight the unreported importance of soil K in fairy ring dynamics affecting microbial communities. This common omission could lead to incorrect conclusions. Hence, the effects of fairy rings on soil should be further tested.

Highlights

- Exchangeable potassium (K) decreased inside the current fairy rings.
- Fairy ring associated changes in PLFA microbial composition were present related to soil K.
- Soil moisture increased in the zones where the rings were 2 years before sampling.
- An environmental stress indicator decreased in those areas.

KEYWORDS

fairy rings, Gram-negative bacteria, Gram-positive bacteria, mountain grasslands, PLFAs, potassium cycle

1 | INTRODUCTION

Soil microbial communities are crucial for a plethora of ecosystem functions and services, including primary production, nutrient cycling, soil carbon storage and soil organic matter decomposition (Aislabie & Deslippe, 2013; Grigulis et al., 2013). Their diversity and composition are driven by factors such as climate, topography, soil properties and vegetation type (de Vries et al., 2012). In addition, at local scales, the diversity and composition of these communities is strongly driven by spatial heterogeneity (Peng et al., 2019), often explained by variations in the physical and chemical properties of soil (i.e., soil water, carbon and nutrient availability; Bardgett & Van Der Putten, 2014). However, some soil microorganisms can be the major drivers of soil spatial patterns at detailed scales, for instance, fairy ring forming fungi.

Fairy rings are circular structures commonly formed by basidiomycete fungi growing radially through the soil (Caesar-TonThat et al., 2013). They can be classified into three types according to their effects on vegetation (Shantz & Piemeisel, 1917). Type-I rings consist of dead or damaged vegetation; type II rings are constituted by exuberant and tall plants; and type III rings do not have visible effects on the vegetation, although the basidiocarps can be observed (Griffith & Roderick, 2008). Fairy rings are a common phenomenon in a wide variety of ecosystems, including forests, grasslands, crops, dunes and turfgrasses (Oudemans et al., 2008; Bonanomi et al., 2013).

Approximately 50 fungi species included in 17 different genera and 14 families have been reported to form fairy rings (Couch, 1962). Previous studies have focussed on one or a few fungal species causing fairy rings, mainly *Agaricus spp.* or *Marasmius odeades* (Bonanomi et al., 2013). This makes their conclusions difficult to generalise (Marí, 2017), especially when considering that fairy ring effects on soil properties may differ depending on the fungal species involved (Yang et al., 2019). Moreover, most studies have considered only fairy rings when fruiting bodies are present, while the works of Marí (Marí, 2017; Marí et al., 2020) showed how type II fairy rings with absent fruiting bodies can have effects on the diversity of microbial communities. These kinds of fairy rings deserve attention, since in this case there is not a clearly predominant fungus species in the soil that can be attributed to fairy ring formation (Marí et al., 2020).

Several studies have addressed the fairy ring associated patterns of different ecosystem components, including plant growth and biodiversity, soil properties and nutrients, and soil microbial communities (Bonanomi et al., 2012; Caesar-TonThat et al., 2013; Yang, Zhang, et al., 2018). Some of the most recent works go a step further and assess the relationship between the patterns of microbial communities and soil variables across fairy rings (Yang et al., 2019; Yang, Zhang, et al., 2018), mainly considering soil pH, moisture, nitrogen and phosphorus. However, those recent studies rarely consider soil nutrients reported to be highly affected by fairy rings, including soil exchangeable potassium (K) and magnesium (Mg) (Edwards, 1988; Fidanza, 2007; but see Zotti et al., 2021).

Phospholipid fatty acid (PLFA) profiling is a tool widely used for assessing soil microbial communities (Bach et al., 2010; Ngosong et al., 2010; Richter et al., 2018). Phospholipid fatty acids are major constituents of cell membranes suitable for analysing soil microbial communities because of their diversity across different groups of groups of microorganisms and rapid degradation after their death (Dubey et al., 2020; Zelles, 1999). Soil PLFA patterns can reflect changes in soil conditions due to differences in agricultural practices, forest management and fertilisation treatments (Fanin et al., 2015; Ngosong et al., 2010; Richter et al., 2018). Surprisingly, to the best of our knowledge, PLFAs have never been used for characterising patterns of the whole soil microbial communities across fairy rings, except Caesar-TonThat et al. (2013) who employed this approach in isolated root-associated soil. The basis of this method is that differences in overall PLFA patterns assessed by multivariate analysis indicate differences in the microbial community (Frostegård et al., 1993). In addition, specific PLFAs are used as biomarkers to assess the biomass of major microbial groups for example, Gram-positive bacteria, Gram-negative bacteria, saprophytic fungi or arbuscular mycorrhizal fungi (AMF) (Kaur et al., 2005). Some ratios between PLFA groups are also used as indicators of shifts in soil carbon channels (i.e., fungal-to-bacteria ratio), habitat factors (i.e., Gram-positive bacteria-to-Gram-negative bacteria ratio) or stress factors (i.e., *iso*-to-*anteiso* fatty acid ratio) (Francisco et al., 2016; Kaneda, 1991).

In this paper, we aimed to expand the knowledge about fairy ring effects on microbial communities, using multivariate techniques to investigate relationships between soil PLFA profiles, soil variables and the

different zones differentiated on fairy ring affected areas: the centre of the circular fairy ring affected area, the zones where the greening belt was placed two- and one-year prior to the sampling year, the zone were the greening belt was located the sampling year, the front of that greening belt and the nearby grassland outside the ring without fairy ring influence. The study site was a montane grassland in the Eastern Pyrenees in the North-Eastern Iberian Peninsula, where fairy rings manifest themselves by inducing plant growth and greening, but where no associated basidiocarps have been found (Marí et al., 2020). The specific questions of this study are:

1. What are the soil variables associated with the different fairy ring zones?
2. How do soil microbial community structure vary through fairy rings, according to soil PLFA pattern characterisation?
3. What are the changes in soil variables associated with changes in the soil microbial community?

2 | MATERIAL AND METHODS

2.1 | Study site

Our study site was La Bertolina, a pastured grassland located in Pla de Busa, in the eastern Pyrenees (42°05′56″N, 1°39′40″E), at 1276 m.a.s.l. La Bertolina has a mean annual temperature of 8.7°C and a mean annual precipitation of 954.8 mm (Ninyerola et al., 2000). The bedrock is limestone with a high stone content of polygenic conglomerates (ICGC; geologic map 1:50000 BG50M_v1r1, 2007, accessed 2015). This grassland is extensively grazed by cattle (0.44 LSU ha^{-1}) from May–June to November. In this montane meso-xerophytic grassland, vegetation is dominated by grasses (*Festuca arundinacea* Schreb., *Poa bulbosa* L., *Dactylis glomerata* L.), although forbs and legumes are often found (*Plantago sp.* pl., *Trifolium pratense* L.).

2.2 | Sampling design

The experiment was performed in May 2017. Previous studies in this grassland area allowed the geo-referencing of 2015 and 2016 fairy rings from aerial images (Figure S1A). We selected six fairy rings, taking into consideration the distance from other rings to avoid interferences, and the continuity of the ring, avoiding incomplete rings whenever possible. Six sampling points were designated in 2017 in a radial transect across each ring (Figure S1B): Centre; R2015 (position of the greening belt of the ring in 2015); R2016 (position of the greening belt of the ring in 2016); R2017 (position of the greening belt of the ring in the sampling year; 2017); Front and Outside the ring in 2017. From this point, we refer to this factor variable as Zone.

2.3 | Soil sampling

At each zone of the six rings, we sampled two soil cores (0–10 cm depth and 9 cm^{-2}). One set of samples was used for PLFA analysis and belowground biomass determination, and the other set of samples was used for analysing soil properties.

2.4 | PLFA analysis

Microbial biomass was determined as the concentrations of PLFAs and neutral lipid fatty acids (NLFAs) using a modified Bligh and Dyer method according to Frostegård et al. (1993). Lipids were extracted from 2 to 4 g of soil (wet weight) by adding 9.2 ml of Bligh-Dyer solvent (chloroform/methanol/citrate buffer at a ratio of 1:2:0.8, pH 4), vortexed and shaken for 2 h. After 10 min centrifugation at 2500 rotations min^{-1}, the solvent was transferred to new tubes and soil was re-extracted with 2.5 ml of Bligh-Dyer solvent by 20 min shaking. Both extracted solvents were combined and the organic and inorganic phases were separated by adding 3.1 citrate buffer and 3.1 ml of chloroform, vortexing and centrifuging (see above). Afterwards, 3 ml of organic phase was transferred to silica acid columns (Chromabond NH_2, Macherey-Nagel, Düren, Germany) conditioned by 2 × 1 ml chloroform. Lipids were eluted into NLFAs, glycolipids and PLFAs using 5 ml chloroform, 20 ml acetone and 5 ml methanol, respectively. Neutral lipid fatty acids and PLFAs were methylated with 1 ml 0.2 M methanolic KOH resulting in fatty acid methylesters (FAMEs). Samples were stored at −20°C.

Fatty acid methylesters were identified by the Sherlock Microbial Identification System Software (MIDI INC., Newark, Delaware, USA) using a 7890A GC-System (Agilent Technologies Inc., Santa Clara, CA, USA) gas chromatograph (GC) and flame ionisation detector equipped with an Ultra 5 capillary column (25 m × 0.2 mm i.d., film thickness 0.33 μm). The temperature program started with 170°C and increased by 28°C min to 288°C, followed by 60°C min^{-1} to 310°C for 40 min. The injection temperature was 250°C and the carrier gas was hydrogen. Quantification was carried out against the internal standard methyl nonadecanoate (19:0) and expressed as nmol PLFAs g^{-1} DW soil.

To verify correct identification of FAMEs (chain length and saturation), samples were additionally

analysed by mass spectrometry using a 7000 GC/MS Triple Quad (Agilent Technologies Inc., Santa Clara, CA, USA), equipped with a HP-5MS capillary column (30 m × 0.25 mm i.d., film thickness 0.25 μm) and helium as carrier gas. The splitless injection was performed at an injection temperature of 240°C. The GC oven temperature started with 40°C (hold time 1 min) and increased by 46°C min^{-1} to 200°C, followed by 5°C min to 238°C, then 120°C min^{-1} to 295°C, and finally 1°C min^{-1} to 300°C, held for 1.65 min. The transfer line temperature was 260°C and a mass range of 45–420 m/z was monitored in scan mode. The FAMEs were identified based on their retention times using external standards of FAME mixtures: Supleco® 37 Component FAME Mix and Bacterial Acid Methyl Ester Mix as well as the standards Me 93, BR 1 and BR 4 from Larodan (Sweden).

The assignment of each FA to each group was done according to Zelles (1999) and is shown in Table S1. We used PLFA 16:1ω5c as a biomarker for arbuscular mycorrhizal fungi despite there are some studies that indicate this should be done with caution, since some PLFA 16:1ω5c can be found in bacteria (Ngosong et al., 2012). However, according to other works, when the ratio of NLFA/PLFA is high, > 1, the contribution of bacterial PLFA 16:1ω5 can be considered low (Olsson, 1999; Zhang et al., 2020), as it was in the average of the six ring zones (Table S4) and in 82% of the samples.

Microbial community structure was assigned by summing the biomarker FAs corresponding to saprotrophic fungi (SF), arbuscular mycorrhizal fungi (AMF), Gram-positive bacteria, Gram-negative bacteria and Actinobacteria. In addition, SF and AMF indicators were summed to obtain total fungal biomass; comparably the biomarker fatty acids for Gram-positive bacteria, Gram-negative bacteria and Actinobacteria were summed as total bacterial biomass. The NLFA 16:1ω5c was used as biomarker for AMF fungal spores (Ngosong et al., 2012). Further, the following general soil microbial PLFA ratios were calculated (see Table S2): fungal-to-bacterial ratio (F/B), Gram-positive bacteria-to-Gram-negative bacteria ratio (Gram+/Gram-), and *iso*-to-*anteiso* FA ratio of the PLFA 17:0 (*i*/*a* 17:0). These are used as measures of microbial response to changes of environmental factors (Kaur et al., 2005; Richter et al., 2018).

2.5 | Soil properties

Soil gravimetric water content was calculated as the difference between the values obtained by weighing soil subsamples before and after drying them at 60°C until constant weight, divided by dry weight (Bilskie, 2001). Soil pH (measured in water), total organic carbon (TC), total nitrogen (TN), $\delta^{13}C$ and $\delta^{15}N$, calcium content (Ca), extractable phosphorus (P), magnesium (Mg) and potassium (K) were measured in air-dried samples (Nelson & Sommers, 1996; Taylor, 2000).

Total carbon (TC) and total nitrogen (TN) content as well as $\delta^{13}C$ and $\delta^{15}N$ of the soil were determined with an elemental auto-analyser coupled to an isotope-ratio mass spectrometer (Flash EA 2000 coupled with Delta V Plus; Thermo Fisher Scientific, Bremen, Germany). For this, the dry and finely ground soil samples were weighed in tin capsules and folded tightly to exclude any atmospheric CO_2 and N_2. Then they were subjected to flash combustion-copper reduction in the elemental analyser with subsequent analysis of C and N stable isotope ratios of CO_2 and N_2. The carbon or nitrogen contents of each sample were determined by peak integration of m/z 44, 45 and 46, and calibrated against elemental standards analysed in the same run. Isotope ratios are expressed as δ-values in per mil (‰), where $\delta = (R\text{sample}/R\text{standard} - 1) \times 1000$, with *R*sample and *R*standard as the isotope ratios ($^{13}C/^{12}C$ or $^{15}N/^{14}N$) of samples and standards, respectively, and reported against Vienna Pee Dee Belemnite (VPDB) ($\delta^{13}C$) and air ($\delta^{15}N$). Besides calibration standards, additional laboratory standard materials were inserted between field samples to monitor the mass spectrometer performance between single autoruns. The overall precision of replicate analyses of samples was <0.1‰ for $\delta^{13}C$ and $\delta^{15}N$. As we obtained a $\delta^{13}C$ range of −26 to −28‰, we can conclude that the content of inorganic carbon in our samples was negligible (Sheldon, 2018; Stevenson et al., 2005). Nevertheless, since we did not differentiate between organic and inorganic carbon, we used the term "total carbon" throughout this work.

Available P was measured by the Olsen method (Vinet & Zhedanov, 1954). Exchangeable Ca, Mg and K were extracted with ammonium acetate (Simard, 1993) and measured with Atomic Absorption Spectroscopy (AAS) (David, 1960).

For calcuation of root biomass, a soil core of 9 cm^2 surface from 0 to 10 cm depth was extracted at each sampling point. In the laboratory, the core was washed and filtered with a 0.2 mm pore size strainer to obtain belowground biomass after oven drying at 60°C until constant weight. Soil variables and their units are summarised in Table S3.

2.6 | Data analysis

2.6.1 | Soil variables across fairy ring zones

All analysis except when it is mentioned, were performed with R version 3.5.2 (R Core Team, 2020), with a

significance level of 95%. We used the lme4 package (Bates et al., 2015) to test the differences between fairy ring zones on each soil variable by using linear mixed effects (LME) models (Lindstrom & Bates, 1988). We modelled each soil variable including Zone as fixed factor and ring identity as random factor, so we controlled other possible landscape patterns on response variables. When the factor Zone was statistically significant (p-value <0.05), a post-hoc test (Tukey test [HSD]) was performed with the emmeans R package (Lenth et al., 2019). Model residuals were graphically evaluated for normal distribution and heteroscedasticity.

2.6.2 | PLFAs across fairy ring zones

We analysed the patterns of microbial communities across fairy ring zones using total PLFA concentration (nmol g^{-1} d.w. in mineral soil) as a measure of microbial biomass, using LME models and following the same approximation as for soil variables. We also considered the calculated PLFA ratios and major microbial group abundances and proportions (%).

To investigate the association of PLFA composition and soil variables and fairy ring zones, redundancy analysis (RDA) was performed with CANOCO 5 (ter Braak & Šmilauer, 2018), using Zone and soil variables as explanatory variables, and ring identity as conditional variable to control possible PLFA patterns related with any landscape factor not measured in the study. We fitted these models with compositional data (%) instead of absolute PLFA concentrations as this improved the explained variance (adjusted R^2) substantially. In addition, we performed another RDA analysis on microbial group composition (including 5 groups: SF, AMF, Gram-positive bacteria, Gram-negative bacteria and Actinobacteria) using the same explanatory variables as for PLFA composition. We log-transformed microbial group composition data, and arcsine-transformed PLFAs composition data to improve the normality of the residuals of RDA models. We calculated the explained variance of both models with adjusted-R^2. We tested single effect test of soil variables on PLFA and microbial group composition, applying a false discovery rate correction to the obtained p-values (Benjamini & Hochberg, 1995).

In addition, we applied another multivariate analysis technique based on classification criteria, the discriminant function analysis (DFA), to investigate how well Zone predicts FA composition; we used the lda function in the MASS package (Vinet & Zhedanov, 2018). We used FA abundances (PLFAs and NLFA 16:1ω5c) as descriptor variables for discrimination, and Zone as the grouping variable, with six levels, one for each fairy ring zone. Before performing the analysis, we checked the normality of FAs by their distribution histograms and Q-Q plots. For this analysis, we selected the FA descriptor variables conforming to the normality assumption, as those without normal distribution were zero-inflated FAs present just in a few plots and in low concentrations. To assign which FAs were responsible for the separation, Pearson correlation coefficients between FAs included in the model and the first two axis obtained were calculated (Richter et al., 2018).

3 | RESULTS

3.1 | Changes in soil properties across fairy ring zones

Soil properties in the mineral layer for each Zone level are shown in Table S3. Soil exchangeable K content peaked in the Outside zones ($F = 3.854$; $p = 0.010$), reaching a mean value of 351 ± 130 mg kg^{-1}, in contrast with the Centre, R2016 and R2017 zones, which were depleted compared to the fairy ring unaffected grassland (mean values: 240 ± 95, 223 ± 55 and 243 ± 52 mg kg^{-1} respectively; Figure 1a). Soil moisture peaked in the R2015 zones (12 ± 1.47 hg g^{-1}), with the lowest mean values in the R2016 and Outside zones (9.12 ± 4.62 and 9.33 ± 2.83 hg g^{-1} respectively; $F = 3.129$, $p = 0.026$; Figure 1b). Total soil carbon tended to show a pattern similar to soil moisture ($F = 2.198$, $p = 0.087$; Figure 1c), while root biomass peaked in the R2017 zones ($F = 2$; $p = 0.115$; Figure 1d). No relevant trends were observed for the remaining soil variables across the ring zones (Figure S2).

3.2 | Changes in PLFA across fairy ring zones

In total, 23 different PLFAs and one relevant NLFA (16:1ω5) were detected in the sampled soils (Table S1). Mean values of total PLFA and major PLFA groups and LME model results are shown in Tables S5 and S6, respectively. There were no significant differences in microbial biomass (i.e., total PLFAs) (Figure S3A; $F = 1.634$, $p = 0.189$) nor in AMF fungal spores ($F = 0.515$, $p = 0.763$; Table S4) across fairy rings.

Only Gram-negative bacteria, among the considered microbial groups (Table S4), showed significant changes across fairy ring zones (Figure S3; $F = 4.237$, $p = 0.007$), being more abundant in the Centre zone of the ring (8.57 ± 1.97 nmol g^{-1} DW) than in the R2015, R2016 and R2017 zones (6.205 ± 1.28, 5.81 ± 1.01 and 5.79 ± 1.69 nmol g^{-1} DW; Figure S3E).

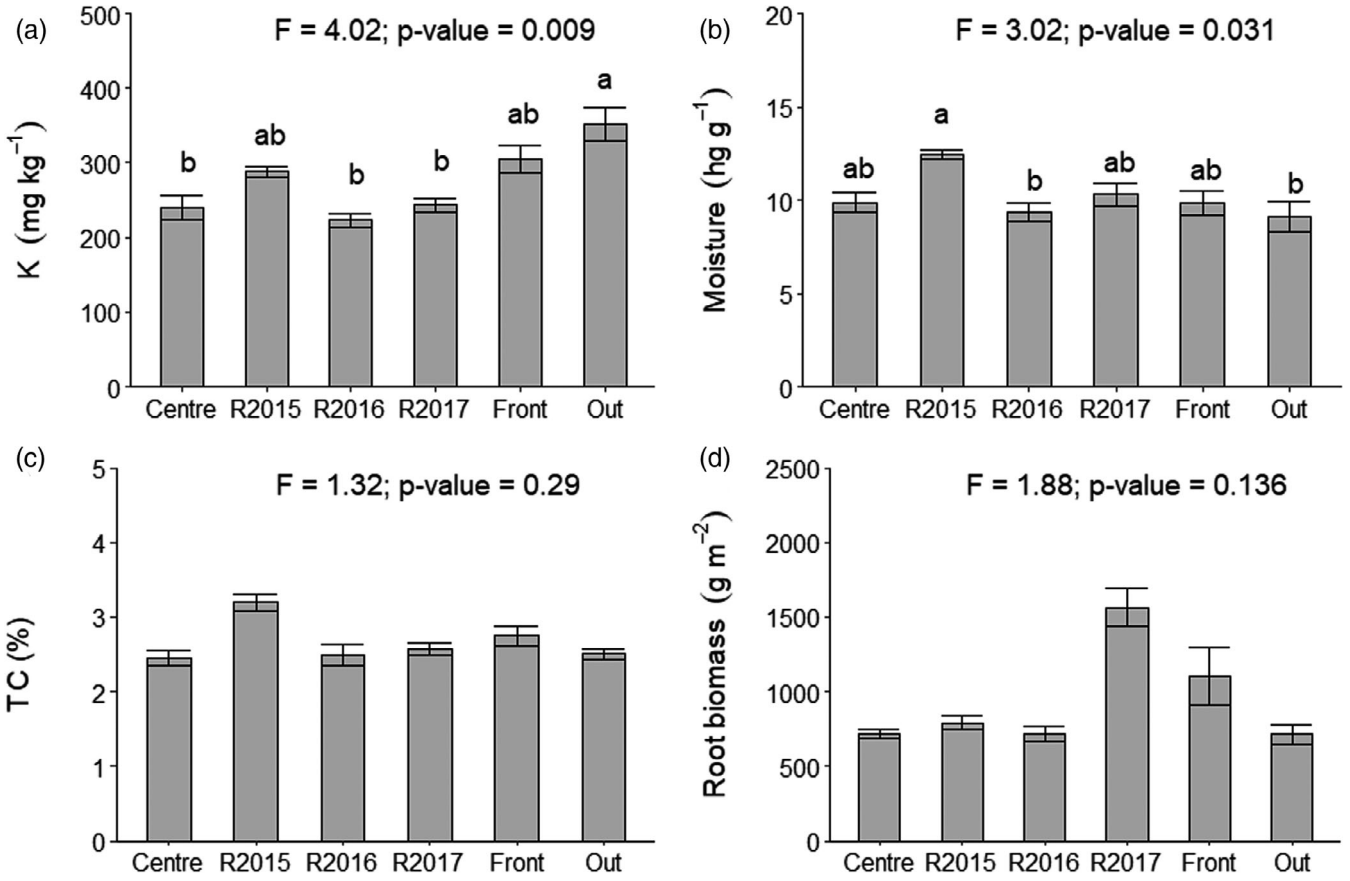

FIGURE 1 Soil K (mg kg^{-1} ± s.e.), soil moisture (hg g^{-1} ± 1 s.e.), total carbon (TC; % ± s.e.) and root biomass (g m^{-2} ± 1 s.e.) in the mineral soil on the 6 zones differentiated on the rings (Centre, R2015, R2016, R2017, front and out). F and *p*-values of mixed effects linear models with ring zone as fixed factor and ring identity as random factor are shown. Different letters indicate significant differences between ring zones (Tukey HSD, $p < 0.05$)

Focusing on the proportion of bacteria from total PLFAs (Table S5), the percentage of bacteria (Figure 2a) was lower in the Outside zones than in the Centre, R2015 and R2017 zones (F = 3.199, $p = 0.023$; mean values: 61.46 ± 5.55 and 66.45 ± 1.17; 66.5 ± 2.08; 66.27 ± 1.64 and 65.3 ± 1.0%); other zones presented intermediate values. Proportions of Gram-positive bacteria from total PLFAs (Figure 2b) was lower in the Outside zones (16.95 ± 5.22%) than in the R2015, R2016 and R2017 zones (F = 3.835, $p = 0.011$; mean values: 23.47 ± 2.02; 22.47 ± 1.84; and 22.35 ± 2.6%). Gram-negative bacteria and Actinobacteria proportions did not show significant differences across ring zones (Figure 2c,d).

Finally, total fungi and saprotrophic fungi proportions tended to peak in the Front zones (F = 2.69; $p = 0.046$ and F = 2.699; $p = 0.045$; respectively; Figure 3a,c; Table S5). We did not find differences in AMF proportion among ring zones (Figure 3b; Table S5).

Concerning PLFA ratios (Table S4), F/B values increased in the Front zone (F = 2.740, $p = 0.043$). The *i*/*a* 17:0 ratio (F = 4.347, $p = 0.006$) showed higher values in the Centre, R2016, Front and Outside zones (0.68 ± 0.088, 0.68 ± 0.086, 0.66 ± 0.024 and 0.68 ± 0.15) than in the R2015 zone (0.43 ± 0.02; Figure 4c) whereas R2017 zone was at an intermediate level. The Gram-positive/Gram-negative bacteria ratio values in the R2015 zones tended to be higher than in the Outside zones (2.39 ± 0.29 and 1.41 ± 0.64, Figure 4a), with the remaining zones in-between (F = 2.371, $p = 0.069$).

3.3 | Relationship between soil variables and microbial group proportions

The RDA extracted three groups, separating Front and Outside from Center, 2016, and 2017 as well as from R2015 (Figure 5). RDA of major microbial groups explained 38.8% of the total variance. Soil exchangeable K and Outside zones were the variables with most relevance (Table 1), explaining 23.9 and 22.9% of the variance. These two variables seemed to relate similarly with the microbial community (Figure 5), being associated

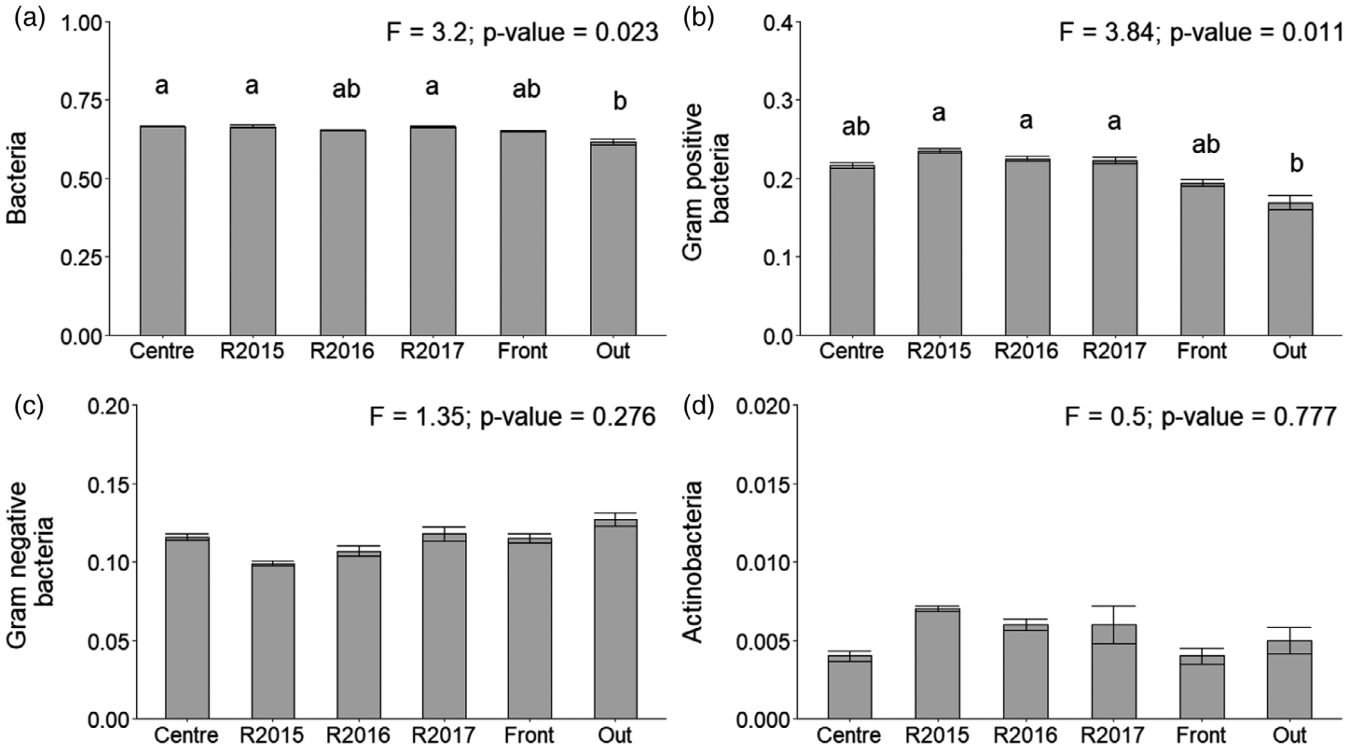

FIGURE 2 Proportions of PLFA markers (± 1 s.e.) of major bacterial groups (bacteria, Gram-positive bacteria, Gram-negative bacteria and Actinobacteria) in mineral soil on the 6 zones differentiated on the rings (Centre, R2015, R2016, R2017, front and out). F and *p*-values of mixed effects linear models with ring zone as fixed factor and ring identity as random factor are shown. Different letters indicate significant differences between ring zones (Tukey HSD, $p < 0.05$)

with high Gram-negative bacteria and low Gram-positive bacteria proportions. Although the Front zones showed less relevance (Figure 5, Table 1), they seemed to be associated with high saprotrophic fungi proportions (Figure 5). In a similar way, AMF was moderately associated with zones inside the ring. R2015 zones were slightly associated with C-to-N ratio, TC and Mg content, and negatively related with proportions of Gram-negative bacteria (Figure 5). The RDA of individual PLFA proportions explained a similar proportion of the variance (28.6%), and supported the main results shown for major groups proportions, that is, the importance of soil exchangeable K and Outside zones (Table S6 and Figure S4). In addition, including the entire PLFA pattern instead of summarising the major groups promoted a greater separation of the mean values of the different ring zones (Figure S4).

3.4 | Changes in microbial community structure across fairy ring zones

The DFA, with soil PLFAs as variables and ring zones as groups, separated the different zones along two roots (Table S7; Figure S5). Root 1 explained 80% of the variance and suggested a wide contrast between the Outside zones and all others. R2017 zones were closest to Outside zones whereas R2016 zones were the most separated ones. Root 1 correlated negatively with a Gram-positive biomarker (*anteiso* 15:0) and one general bacteria marker (16:1ω9c). Thus, Outside zones were differentiated from the zones inside of the ring by a lower Gram-positive bacteral abundance and, in general, bacterial abundance (Figure S5; Table S7), with the largest differences to R2016 zones. The separation along Root 2 was less distinct, explaining 12% of the variance and mainly discriminating Front zones from R2015 (Figure S5). Root 2 was correlated negatively with a saprophytic fungi marker (18:2ω6c) and positively with one general bacteria marker (19:1ω8c) (Table S7), pointing to a relatively higher biomass of saprotrophic fungi in the Front zones in comparison to all other ring zones (Figure S5; Table S7).

4 | DISCUSSION

4.1 | Soil variable changes in fairy ring zones

Exchangeable K and moisture were the two soil parameters responding most strongly to the presence of fairy

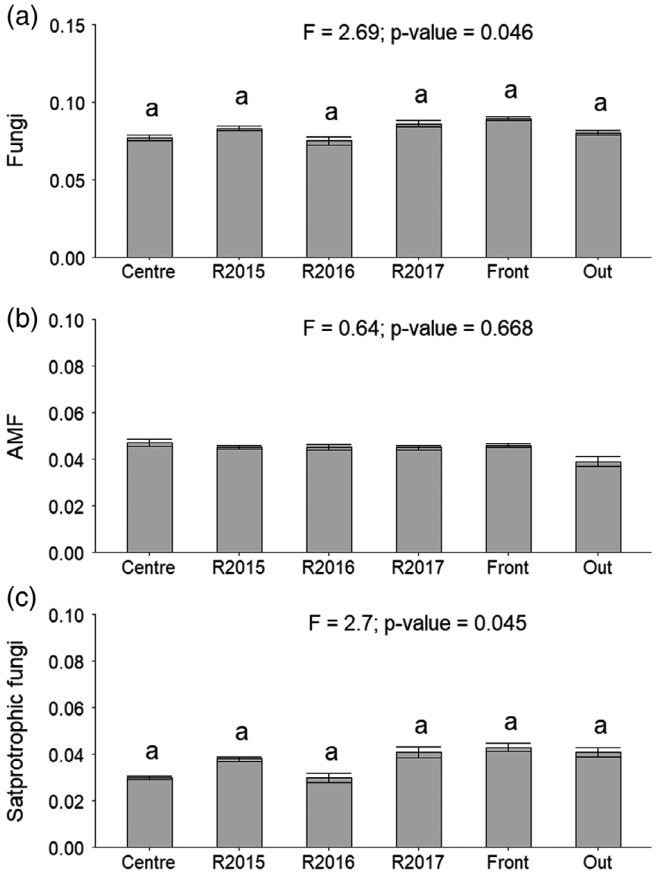

FIGURE 3 Proportions (± 1 s.e.) of major fungal groups (fungi, AMF, saprotrophic fungi) in mineral soil on the 6 zones differentiated on the rings (Centre, R2015, R2016, R2017, front and outside). F and *p*-values of mixed effects linear models with ring zone as fixed factor and ring identity as random factor are shown. Different letters indicated significant differences between ring zones (Tukey HSD, $p < 0.05$). If all letters are the same, post-hoc test did not find significant differences between groups

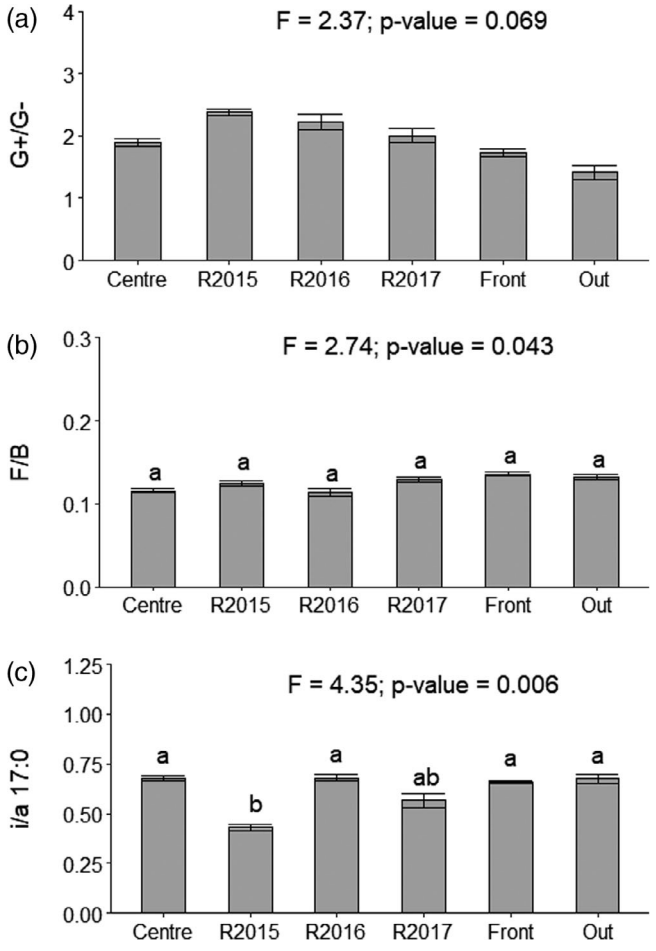

FIGURE 4 Microbial indicators (PLFA ratios ±1 s.e.) in the mineral soil on the 6 zones differentiated on the rings (Centre, R2015, R2016, R2017, front and outside). The ratios of Gram-positive bacteria-to-Gram-negative bacteria (G+/G−); fungi to bacteria (F/B); and *iso* to *anteiso* of the PLFA 17.0 (*i*/*a*17:0) are shown. F and *p*-values of mixed effects linear models with ring zone as fixed factor and ring identity as random factor are shown. Different letters indicated significant differences between ring zones (Tukey HSD, $p < 0.05$). If all letters are the same, post-hoc test did not find significant differences between groups

rings (Figure 1). Potassium, in addition to N and P, is a highly important nutrient for fairy ring fungi and other basidiomycetes (Edwards, 1984, 1988). Our results in La Bertolina suggest that the consequences of fairy ring activity could be more severe for soil K than for P and N (Figures 1 and S2; Table S3). Our results contrast with a recent study about the fairy ring forming fungus *Calocybe gambosa* (Zotti et al., 2021) that reported an increase of exchangeable K at the zones of passage of the fairy rings, but the levels out and inside the ring were statistically similar. In agreement with our results, Edwards (1984) found a sharp decrease of exchangeable K inside fairy rings, much higher than that observed for soil N or P. However, Edwards also detected an increase of soil K under the greening belt zone, which was absent in our results. The fairy ring passage could leave more long-term footprints on soil K than in N or P, since the last two are mostly part of complex molecular structures in soil organic matter whereas K is always available in soluble form (McGrath et al., 2014), being more easily leached than N or P (Sardans & Peñuelas, 2015).

Surprisingly, soil moisture peaked in the R2015 zones (Figure 1b). Fairy rings often produce decreases in soil moisture, either in the greening belt (Yang et al., 2019) or in a wide area inside the ring affected area (Bonanomi et al., 2012), which have been attributed to soil drought conditions induced by the fairy ring fungi (Fidanza, 2007). However, we only observed a significant increase in soil moisture where the rings had been located 2 years before the sampling year. The R2015 zones also showed a tendency for higher values of TC. We suggest that further studies addressing

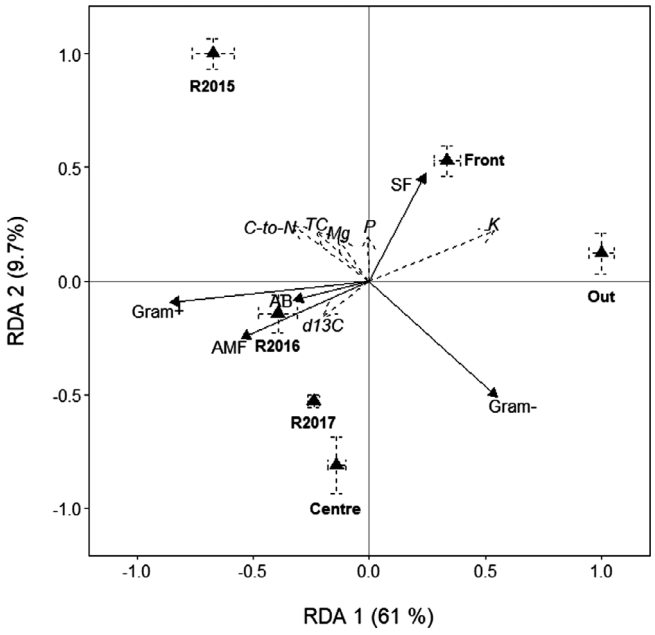

FIGURE 5 Redundancy analysis (RDA) of the association between environmental variables and ring zone with microbial grouping pattern (%) full arrows indicate microbial group scores: AB: Actinobacteria; AMF: Arbuscular mycorrhizal fungi; Gram +: Gram-positive bacteria; Gram-: Gram-negative bacteria; SF: Saprophytic fungi. Dashed arrows indicate soil variable scores: Ca: Calcium; C-to-N: C-to-N ratio; $\delta^{13}C$; K: Potassium; Mg: Magnesium; moisture: Soil moisture; P: Available phosphorus; pH: Soil pH; TC: Total carbon. Triangles indicate fairy ring zone centroids scores (Centre; R2015; R2016; R2017, front and outside) with their standard errors. Site centroids were scaled to 1 on their maximum values for a better representation. Variables with small values (both factor scores between −0.14 and 0.14) are not shown

TABLE 1 Single effects test of soil properties and fairy ring zones on microbial group composition

	Microbial group composition		
	Explained var. (%)	F	*p*-value
Ring zones			
Centre	1.5	0.4	0.87
R2015	9.6	3.0	0.33
R2016	4.2	1.2	0.80
R2017	2.7	0.8	0.85
Front	3.3	0.9	0.80
Out	22.9	8.3	0.04
Soil properties			
Belowground biomass	1.5	0.4	0.87
Ca	0.5	0.1	0.91
C-to-N	9.7	3.0	0.33
$\delta^{13}C$	3.7	1.1	0.80
$\delta^{15}N$	1.2	0.4	0.88
K	23.9	8.8	0.04
Mg	1.9	0.5	0.87
Moisture	0.5	0.1	0.91
P	0.6	0.2	0.91
pH	0.6	0.2	0.91
TN	1.8	0.5	0.87
TC	5	1.5	0.80

relationships between fairy rings and soil or vegetation should consider the past fairy ring spatial dynamics in their sampling. Our results suggest that carrying out regularly spaced transects inside the rings as in previous works (Zotti et al., 2020) could mask some spatial patterns of fairy rings in grassland ecosystems.

Another noticeable result was the clear absence of differences between fairy ring zones in the remaining soil parameters (Figure S2). The lack of differences on soil pH could be caused by the calcareous nature of this grassland (Marí, 2017), providing a strong buffering capacity and resistance to soil acidification (Brady & Weil, 2017; Kirk et al., 2010), and potentially disabling the biochemical effects of the microbial activity in the front and R2017 zones (Marí, 2017). Decreases in soil pH under the lush vegetation belt zones of fairy rings (Bonanomi et al., 2012; Yang, Zhang, et al., 2018; Zotti et al., 2021) had been related to an increase in the solubility of mineral nutrients (Gramss et al., 2005). However, Yang et al. (2019) report an increase in soil pH in lush fairy ring zones in a grassland with different climate and soil conditions. Soil pH is the "soil master variable" which conditions soil nutrients and their availability (McGrath et al., 2014). Hence, the absence of soil pH differences between ring zones in our study could be behind the homogeneity of soil nutrients through fairy ring zones.

Concerning soil nutrients, our results are especially surprising for soil N and/or soil available P, the nutrients most commonly reported to be affected by fairy rings in recent studies (Caesar-TonThat et al., 2013; Yang, Li, et al., 2018). Total N usually decreases after fungal passage (Bonanomi et al., 2012; Edwards, 1984; Fisher, 1977; Yang, Li, et al., 2018) and available P often increased in the front zones or in the soils under the affected greening belts (Caesar-TonThat et al., 2013; Yang et al., 2019; Yang, Li, et al., 2018). The lack of variation of soil total N and P could be explained by three non-exclusive hypotheses. First, Edwards (1988) proposed that fairy ring fungi could have assimilated soil total N and that the lack of differences is caused by the incapability of soil analyses to distinguish between N in the mycelium and in the soil. We are reluctant to accept this hypothesis because changes in soil total N have been observed in previous

works following similar soil analysis methodologies as ours (Bonanomi et al., 2012; Yang, Zhang, et al., 2018). Second, considering that fairy ring effects in soil tend to decrease with time since fungi have taken up soil nutrients (Fisher, 1977; Yang, Li, et al., 2018) the similar values of soil N and available P across fairy ring zones could be because the nutrient uptake of the fairy ring fungi happened before the sampling date. However, our sampling was performed when the ring effects in the vegetation were most visible, similar to other studies on fairy rings (Marí et al., 2020; Yang, Li, et al., 2018; Zotti et al., 2020). Finally, nutrient requirements of fairy ring fungi in La Bertolina could be lower than those in other locations, due to the absence of fruiting bodies, which normally require a high nutrient investment (Gençcelep et al., 2009; Moore et al., 2008).

4.2 | Microbial community changes across fairy ring zones

Fairy rings in La Bertolina affected mainly the structure and composition of microbial communities (Figures 2, 3 & S3), rather than total PLFAs (Figure S3A), an indicator of microbial biomass (Joergensen & Wichern, 2008; Klamer & Bååth, 2004). Our results partially contrast with Bonanomi et al. (2012), who observed that fungal passage may favour certain microbial groups, but reduced the total microbial population.

Focusing on the major microbial groups, the most conspicuous differences on microbial communities across fairy rings where those concerning Gram-positive bacteria and Gram-negative bacteria. These results suggested that fairy rings affected soil bacteria through altering nutrient dynamics, since it is well known that some Gram-negative bacteria tend to proliferate in nutrient rich conditions (Griffiths et al., 1998; Miller et al., 1990), and are frequent in root associated soils, whereas Gram-positive bacteria are commonly oligotrophic specialists and more typical of bulk soils (Kramer & Gleixner, 2008; Ramesh et al., 2012).

Our analysis showed that the proportion of Gram-positive bacteria increased inside the ring-affected areas, while the abundance of Gram-negative bacteria decreased during the ring passage, recovering to previous high values in the ring centre (Figures 2b & S3E). There were no sharp differences for any of those microbial groups in the greening belts or the Front zones. These results partially contrast with Caesar-TonThat et al. (2013), who reported a slight peak of Gram-negative bacteria proportions in the greening belt zone when analysing proportion of cultivable bacteria PLFA in root-associated soils. Similarly, increases in copiotrophic taxa sequences in soils under the greening belts are frequently found in fairy ring metabarcoding studies (Marí, 2017; Oh & Lim, 2018; Yang et al., 2019; Zotti et al., 2020, 2021).

We expected higher fungal predominance in Front zones since fungi are supposed to be most abundant in the zones where the mineralizing activity of the fungus occurs (Bonanomi et al., 2012; Caesar-TonThat et al., 2013). The PLFA proportions of total fungi and saprotrophic fungi as well as the F/B ratio tended to reach their maximum values at the Front zones. However, although in line with the rest of our results in the Front and R2017 zones, these tendencies were weak (Figures 3 & 4b). Saprotrophic fungi were weakly associated with the Front zones in the RDA analysis (Figure 5) and the LDA analysis confirmed this result, separating Front zones on the second root, and Pearson's correlations suggested that a higher biomass of saprotrophic fungi explained this pattern (Figure S5; Table S7). The most recent studies reporting fungi metabarcoding results show variable results on how soil fungal communities can be affected by fairy ring passage (Marí et al., 2020; Zotti et al., 2020), which highlights the heterogeneity of the ecological processes that fairy ring fungi can unleash.

In a study carried out in the same location as the present study, Marí et al. (2020) found an increase of fungal diversity in the front zones that was maintained in all the area inside the ring. No particular fungal species dominated in the front zones, which combined with the absence of basidiocarps, made the identification of the fungi inducing the fairy rings impossible. On the other hand, in a study located in central Italy, Zotti et al. (2020) reported a decrease in soil fungal diversity in the front zone, since the fairy ring forming fungus *Agaricus arvensis* was by far the dominant fungus in those areas. In that case, the fungal community was practically restored after the fungal passage (similarly to Lian et al. (2006)). Interestingly, they found that AMF were associated with the inner zones of the rings (Zotti et al., 2020). Although we did not find significant differences in PLFA of AMF among fairy ring zones (Figure 3b), our RDA analysis also showed a moderate association between this PLFA indicator and the inner zones of the ring (Figure 5).

Arbuscular mycorrhizal fungi might have a role in the growth and lushness of vegetation promoted by fairy rings (Zotti et al., 2020), as they would facilitate P absorption uptake by plants (Nouri et al., 2014). Arbuscular mycorrhizal fungi also have been described as facilitators of plant K nutrition (Garcia & Zimmermann, 2014). Considering our results about AMF with caution, we suggest that further studies about the role of AMF on fairy rings should consider both P and K, taking into account the importance the latter appears to have in fairy rings development (Edwards, 1984).

4.3 | Relationship between the changes of soil variables and microbial communities in fairy ring zones

The observed changes in microbial communities indicate possible changes in soil nutrient conditions (Orwin et al., 2018). The RDA analysis pointed to the decrease in exchangeable soil K values inside the ring as the variable associated with the Gram-positive bacteria increase and Gram-negative bacteria decrease inside the ring (Figure 5; Table 1). Hence, exchangeable soil K was a potential intermediate driver of the observed patterns of microbial communities across fairy ring zones. This could be a key finding for understanding the effects of fairy rings on microbial communities, since soil K is almost never included in the most recent fairy ring studies (Caesar-TonThat et al., 2013; Yang et al., 2019; Yang, Zhang, et al., 2018). Two decades ago, Edwards (Edwards, 1984, 1988) noted that K was the soil nutrient most decreased by fairy ring passage. However, of the recent studies only Zotti et al. (2021) considered soil exchangeable K, but in this case this variable was not associated with soil microbial communities. We consider that this negligence of soil K could lead to incomplete conclusions about the role of soil nutrients on fairy ring dynamics, as some fairy ring effects on plant or microbial communities that have been attributed to changes in compounds including available P or N (Caesar-TonThat et al., 2013; Yang et al., 2019; Yang, Zhang, et al., 2018) could be partially caused by changes on soil exchangeable K (Fay et al., 2015).

Potassium is a mineral nutrient of key importance for almost any living organism, and it is crucial for microbial enzyme activity and osmotic equilibrium (Luo et al., 2016; Madigan et al., 2015). In laboratory assays, the single capacity of exchangeable soil K changes for affecting microbial communities has been recently demonstrated in a microcosm experiment (Nicolitch et al., 2019). Our work provided a field example of soil exchangeable K being the most explicative nutrient of the differences in microbial community structure between different zones of the fairy ring zones. The K cycle is of main ecological interest since the ecological dynamics of K remain poorly understood (Sardans & Peñuelas, 2015). Hence, if the impact of fairy rings on exchangeable soil K results to be confirmed in further studies, grassland fairy rings could be an interesting subject for studying the K cycle, and its interactions with N, P, microorganism and plant communities (Yang et al., 2019).

In previous works, changes in bacterial communities under the lush vegetation belt zones were associated with high inorganic N (instead of total N) and available P conditions (Caesar-TonThat et al., 2013; Yang, Zhang, et al., 2018). We did not observe significant differences on available P (Figure S2C). Although we did not measure inorganic N (because we did not find any difference in soil inorganic N content between ring zones in previous sampling campaigns; data not shown), the PLFA patterns obtained suggest that there was no increase in soil inorganic N in the R2017 or the Front zones (Wang et al., 2020), or at least these enhancements were not related with microbial communities, maybe because plants could outcompete microorganisms in N uptake (Wang et al., 2020).

Results from a sampling carried out in 2015 (Marí, 2017) in the same rings studied here reported peaks of DNA proportions of some copiotrophic bacteria in greening belt areas, being indicative of increases of some nutrients (Yang, Zhang, et al., 2018). This suggests that different patterns of soil nutrients and microorganisms can be found even in the same ring-affected grassland.

Apart from Gram-positive baceria and Gram-negative bacteria, fairy ring zones also exhibited significant differences in their *i*/*a*17:0 ratio, which noticeably decreased in the R2015 zones. This suggest environmental stress may decrease in R2015 zones (Muhammad et al., 2014). Differences in *iso*-to-*anteiso* ratios are commonly attributed to differences in temperature, soil moisture or nutrients (Bach et al., 2010; Siddikee et al., 2016). Considering the local scale of our study, we suggest that the last two factors might explaing this pattern, since temperature differences should occur at broader scales (Richter et al., 2018). In fact, the R2015 zones were not only the highest in moisture content (Figure 1b) but also those with the highest exchangeable K content among the zones inside the ring-affected areas (Figure 1a). Changes in soil moisture can drive microbial communities through the alteration of soil physicochemical properties (Li et al., 2019). However, in our case soil moisture did not appear significantly associated to the microbial group indicators nor the whole microbial community (Figures 5 & S4). These results suggest that soil bacteria could adapt themselves to the different moisture conditions across fairy ring zones by changing their PLFA *iso*-to-*anteiso* ratio to modify the permeability of their membranes, thus preserving the structure of microbial community (Santos et al., 2019).

5 | CONCLUSIONS

Soil exchangeable K was the soil variable most conspicuously affected by fairy rings, decreasing inside the ring zones compared to the unaffected grassland. This pattern seemed to explain the association of Gram-negative bacteria with the Outside zones, and the increase in Gram-positive bacteria proportions in the zones inside the ring. Soil moisture was higher in the zones where the greening

belts of the fairy ring had been 2 years before sampling. This pattern was coincident with a decrease in microbial environmental stress, indicated by the *i*/*a*17:0 ratio. This result suggest that past spatial fairy ring dynamics could have some effect on present soil properties and the spatial variability of microbial communities, although more research is needed to verify and to characterise this pattern. In contrast with previous studies, no difference on soil N or P across fairy rings was found. Only soil fungi showed an increasing trend in the Front zones. Finally, our results suggest that further studies should focus on the role of AMF in fairy ring dynamics and their potential facilitation of plant nutrient uptake not only of soil P but also soil K.

AUTHOR CONTRIBUTIONS

Antonio Rodríguez participated in field sampling, performed the PLFA extraction, designed the statistical procedure, carried out the statistical analyses and wrote the original draft. Mercedes Ibáñez was responsible for field sampling and soil lab. She has reviewed the draft. Roland Bol contributed the C and N isotope analysis of soil samples, and reviewed and edited the manuscript. Nicolas Brüggemann contributed the C and N isotope analysis of soil samples, and reviewed and edited the manuscript. Agustín Lobo contributed to image processing and geolocalization of fairy rings in this study, and read and revised the paper. Liliane Ruess analyzed the soil PLFAs and validated the related GC-MS ion pattern. She reviewed and edit the manuscript draft. M.-Teresa Sebastià contributed to the conception, design and development of the fairy rings study, acquired funding, supervised the development of the paper, and read and reviewed the drafts.

ACKNOWLEDGEMENTS

We would like to express our thanks to the many people who collaborated in fieldwork, sample processing and data analysis. This work was funded by the Spanish Science Foundation FECYT- MINECO (projects BIOGEI: GL2013-49142-C2-1-R; and IMAGINE: CGL2017-85490-R), the Universitat de Lleida (PhD Fellowship to AR), and COST Action ES1406 for a Short Term Scientific Mission to AR. The ARAID foundation is acknowledged for support to Juan José Jimenez.

DATA AVAILABILITY STATEMENT

The data that support the findings of this study are available from the corresponding author upon reasonable request.

ORCID

Antonio Rodríguez https://orcid.org/0000-0002-0536-9902
Mercedes Ibáñez https://orcid.org/0000-0003-0917-6232
Roland Bol https://orcid.org/0000-0003-3015-7706
Nicolas Brüggemann https://orcid.org/0000-0003-3851-2418
Agustín Lobo https://orcid.org/0000-0002-6689-2908
Juan José Jimenez https://orcid.org/0000-0003-2398-0796
Liliane Ruess https://orcid.org/0000-0001-8061-6208
M.-Teresa Sebastià https://orcid.org/0000-0002-9017-3575

REFERENCES

Aislabie, J., & Deslippe, J. R. (2013). Soil microbes and their contribution to soil services. In J. R. Dymond (Ed.), *Ecosystem services in New Zealand - conditions and trends* (pp. 143–161). Manaaki Whenua Press.

Bach, E. M., Baer, S. G., Meyer, C. K., & Six, J. (2010). Soil texture affects soil microbial and structural recovery during grassland restoration. *Soil Biology and Biochemistry*, *42*, 2182–2191. https://linkinghub.elsevier.com/retrieve/pii/S0038071710003020. Accessed: 7/10/2019.

Bardgett, R. D., & Van Der Putten, W. H. (2014). Belowground biodiversity and ecosystem functioning. *Nature*, *515*, 505–511. https://doi.org/10.1038/nature13855

Bates, D., Mächler, M., Bolker, B., & Walker, S. (2015). Fitting linear mixed-effects models using {lme4}. *Journal of Statistical Software*, *67*, 1–48.

Benjamini, Y., & Hochberg, Y. (1995). Controlling the false discovery rate: A practical and powerful approach to multiple testing. *Journal of the Royal Statistical Society: Series B: Methodological*, *57*, 289–300. https://doi.org/10.1111/j.2517-6161.1995.tb02031.x. Accessed: 30/9/2019.

Bilskie, J. (2001). Soil water status: Content and potential. Campbell scientific Inc. *App. Note 2S-1*, *1784*, 84321, https://s.campbellsci.com/documents/us/technical-papers/soilh20c.pdf. Accessed: 20/9/2019

Bonanomi, G., Incerti, G., & Allegrezza, M. (2013). Assessing the impact of land abandonment, nitrogen enrichment and fairy-ring fungi on plant diversity of Mediterranean grasslands. *Biodiversity and Conservation*, *22*, 2285–2304.

Bonanomi, G., Mingo, A., Incerti, G., Mazzoleni, S., & Allegrezza, M. (2012). Fairy rings caused by a killer fungus foster plant diversity in species-rich grassland. *Journal of Vegetation Science*, *23*, 236–248. https://doi.org/10.1111/j.1654-1103.2011.01353.x. Accessed: 19/9/2019.

Brady, N., & Weil, R. (2017). Soil water: Characteristics and behavior. In N. Brady & R. Weil (Eds.), *The nature and properties of soils* (15th ed., pp. 243–249). Pearson.

Caesar-TonThat, T. C., Espeland, E., Caesar, A. J., Sainju, U. M., Lartey, R. T., & Gaskin, J. F. (2013). Effects of Agaricus lilaceps fairy rings on soil aggregation and microbial community structure in relation to growth stimulation of Western wheatgrass (Pascopyrum smithii) in eastern Montana rangeland. *Microbial Ecology*, *66*, 120–131. https://doi.org/10.1007/s00248-013-0194-3. Accessed: 19/9/2019.

Couch, H. B. (1962). *Diseases of Turfgrasses*. Rheinhold Publishing Corp.

David, D. J. (1960). The determination of exchangeable sodium, potassium, calcium and magnesium in soils by atomic-absorption spectrophotometry. *The Analyst*, *85*, 495–503.

de Vries, F. T., Manning, P., Tallowin, J. R. B., Mortimer, S. R., Pilgrim, E. S., Harrison, K. A., Hobbs, P. J., Quirk, H., Shipley, B., Cornelissen, J. H. C., Kattge, J., & Bardgett, R. D. (2012). Abiotic drivers and plant traits explain landscape-scale patterns in soil microbial communities. *Ecology Letters*, *15*, 1230–1239.

Dubey, R. K., Tripathi, V., Prabha, R., Chaurasia, R., Singh, D. P., Rao, C. S., El-Keblawy, A., & Abhilash, P. C. (2020). Methods for exploring soil microbial diversity. In R. K. Dubey, V. Tripathi, R. Prabha, R. Chaurasia, D. P. Singh, C. S. Rao, A. El-Keblawy, & P. C. Abhilash (Eds.), *Unravelling the soil microbiome: Perspectives for environmental sustainability* (pp. 23–32). Springer International Publishing.

Edwards, P. J. (1984). The growth of fairy rings of Agaricus Arvensis and their effect upon grassland vegetation and soil. *The Journal of Ecology*, *72*, 505.

Edwards, P. J. (1988). Effects of the fairy ring fungus Agaricus arvensis on nutrient availability in grassland. *New Phytologist*, *110*, 377–381. https://doi.org/10.1111/j.1469-8137.1988.tb00275.x. Accessed: 3/10/2019.

Fanin, N., Hättenschwiler, S., Schimann, H., & Fromin, N. (2015). Interactive effects of C, N and P fertilization on soil microbial community structure and function in an Amazonian rain forest. *Functional Ecology*, *29*, 140–150.

Fay, P. A., Prober, S. M., Harpole, W. S., Knops, J. M. H., Bakker, J. D., Borer, E. T., Lind, E. M., MacDougall, A. S., Seabloom, E. W., Wragg, P. D., Adler, P. B., Blumenthal, D. M., Buckley, Y. M., Chu, C., Cleland, E. E., Collins, S. L., Davies, K. F., Du, G., Feng, X., … Yang, L. H. (2015). Grassland productivity limited by multiple nutrients. *Nature Plants*, *1*, 1–5. www.nature.com/natureplants. Accessed: 15/7/2020.

Fidanza, M. A. (2007). Characterization of soil properties associated with type-I fairy ring symptoms in turfgrass. *Biologia*, *62*, 533–536. http://www.aasl.psu.edu/. Accessed: 23/10/2019.

Fisher, R. F. (1977). Nitrogen and phosphorus mobilization by the fairy ring fungus, Marasmius oreades (bolt.) fr. *Soil Biology and Biochemistry*, *9*, 239–241. https://www.sciencedirect.com/science/article/pii/0038071777900281. Accessed: 3/10/2019.

Francisco, R., Stone, D., Creamer, R. E., Sousa, J. P., & Morais, P. V. (2016). European scale analysis of phospholipid fatty acid composition of soils to establish operating ranges. *Applied Soil Ecology*, *97*, 49–60. https://www.sciencedirect.com/science/article/pii/S0929139315300809. Accessed: 26/9/2019.

Frostegård, Å., Bååth, E., & Tunlio, A. (1993). Shifts in the structure of soil microbial communities in limed forests as revealed by phospholipid fatty acid analysis. *Soil Biology and Biochemistry*, *25*, 723–730. https://www.sciencedirect.com/science/article/pii/003807179390113P. Accessed: 18/3/2019.

Garcia, K., & Zimmermann, S. D. (2014). The role of mycorrhizal associations in plant potassium nutrition. *Frontiers in Plant Science*, 5–337. https://doi.org/10.3389/fpls.2014.00337. Accessed: 24/7/2020.

Gençcelep, H., Uzun, Y., Tunçtürk, Y., & Demirel, K. (2009). Determination of mineral contents of wild-grown edible mushrooms. *Food Chemistry*, *113*, 1033–1036.

Gramss, G., Voigt, K.-D. D., & Bergmann, H. (2005). Factors influencing water solubility and plant availability of mineral compounds in the tripartite fairy rings of Marasmius oreades (BOLT.: FR.) FR. *Journal of Basic Microbiology*, *45*, 41–54. https://doi.org/10.1002/jobm.200410459. Accessed: 3/10/2019.

Griffith, G. W., & Roderick, K. (2008). Chapter 15 saprotrophic basidiomycetes in grasslands: Distribution and function. *British Mycological Society Symposia Series*, *28*, 277–299.

Griffiths, B. S., Ritz, K., Ebblewhite, N., & Dobson, G. (1998). Soil microbial community structure: Effects of substrate loading rates. *Soil Biology and Biochemistry*, *31*, 145–153. https://www.sciencedirect.com/science/article/pii/S0038071798001175. Accessed: 7/10/2019.

Grigulis, K., Lavorel, S., Krainer, U., Legay, N., Baxendale, C., Dumont, M., Kastl, E., Arnoldi, C., Bardgett, R. D., Poly, F., Pommier, T., Schloter, M., Tappeiner, U., Bahn, M., & Clément, J.-C. (2013). Relative contributions of plant traits and soil microbial properties to mountain grassland ecosystem services. *Journal of Ecology*, *101*, 47–57. https://doi.org/10.1111/1365-2745.12014. Accessed: 27/1/2020.

Joergensen, R. G., & Wichern, F. (2008). Quantitative assessment of the fungal contribution to microbial tissue in soil. *Soil Biology and Biochemistry*, *40*, 2977–2991. https://www.sciencedirect.com/science/article/pii/S0038071708002915. Accessed: 16/10/2019.

Kaneda, T. (1991). Iso- and anteiso-fatty acids in bacteria: Biosynthesis, function, and taxonomic significance. *Microbiological Reviews*, *55*, 288–302.

Kaur, A., Chaudhary, A., Kaur, A., Choudhary, R., & Kaushik, R. (2005). Phospholipid fatty acid - a bioindicator of environment monitoring and assessment in soil ecosystem. *Current Science*, *89*, 1103–1112.

Kirk, G. J. D., Bellamy, P. H., & Lark, R. M. (2010). Changes in soil pH across England and Wales in response to decreased acid deposition. *Global Change Biology*, *16*, 3111–3119. h10.1111/j.1365-2486.2009.02135.x. Accessed: 14/7/2020.

Klamer, M., & Bååth, E. (2004). Estimation of conversion factors for fungal biomass determination in compost using ergosterol and PLFA 18:2ω6,9. *Soil Biology and Biochemistry*, *36*, 57–65. https://www.sciencedirect.com/science/article/pii/S0038071703002931. Accessed: 16/10/2019.

Kramer, C., & Gleixner, G. (2008). Soil organic matter in soil depth profiles: Distinct carbon preferences of microbial groups during carbon transformation. *Soil Biology and Biochemistry*, *40*, 425–433.

Lenth, R., Singmann, H., Love, J., Buerkne, P. & Herve, M. (2019). *Package 'emmeans.'* https://cran.r-project.org/web/packages/emmeans/. Accessed: 18/3/2019

Li, J., An, C., Shang, J., Zhao, T., Zhang, Q., Yang, X., Ren, C., Huang, D., Liu, K., & Shao, X. (2019). Spatial patterns in soil physicochemical and microbiological properties in a grassland adjacent to a newly built lake. *MicrobiologyOpen*, *8*, 1–13. https://doi.org/10.1002/mbo3.912. Accessed: 7/10/2019.

Lian, C., Narimatsu, M., Nara, K., & Hogetsu, T. (2006). Tricholoma matsutake in a natural Pinus densiflora forest: Correspondence between above- and below-ground genets, association with multiple host trees and alteration of existing ectomycorrhizal communities. *New Phytologist*, *171*, 825–836.

Lindstrom, M. J., & Bates, D. M. (1988). Newton—Raphson and EM algorithms for linear mixed-effects models for repeated-measures data. *Journal of the American Statistical Association*, *83*, 1014–1022.

Luo, X., Fu, X., Yang, Y., Cai, P., Peng, S., Chen, W., & Huang, Q. (2016). Microbial communities play important roles in modulating paddy soil fertility. *Scientific Reports*, *6*, 20326. https://doi.org/10.1038/srep20326. Accessed: 16/7/2020.

Madigan, M. T., Martinko, J. M., & Parker, J. (2015). Brock biology of microorganisms. In *Pearson/Benjamin Cummings*. https://books.google.es/books?id=ynWoIAAACAAJ

Marí, T. (2017). *Changes in soil biodiversity and activity along management and climatic gradients*. University of Lleida.

Marí, T., Castaño, C., Rodríguez, A., Ibáñez, M., Lobo, A., Sebastià, M. T., & Sebastià, T. (2020). Fairy rings harbor distinct soil fungal communities and high fungal diversity in a montane grassland. *Fungal Ecology*, *47*, 100962.

McGrath, J. M., Spargo, J., & Penn, C. J. (2014). Soil fertility and plant nutrition. In *Encyclopedia of agriculture and food systems* (pp. 166–184). Elsevier.

Miller, H. J., Liljeroth, E., Henken, G., & van Veen, J. A. (1990). Fluctuations in the fluorescent pseudomonad and actinomycete populations of rhizosphere and rhizoplane during the growth of spring wheat. *Canadian Journal of Microbiology*, *36*, 254–258. https://doi.org/10.1139/m90-044. Accessed: 7/10/2019.

Moore, D., Gange, A. C., Gange, E. G., & Boddy, L. (2008). Fruit bodies: Their production and development in relation to environment. In L. Boddy, J. Frankland, & P. van West (Eds.), *Ecology of saprotrophic basidiomycetes* (1st ed., pp. 79–103). Elsevier.

Muhammad, N., Dai, Z., Xiao, K., Meng, J., Brookes, P. C., Liu, X., Wang, H., Wu, J., & Xu, J. (2014). Changes in microbial community structure due to biochars generated from different feedstocks and their relationships with soil chemical properties. *Geoderma*, *226*, 226–227. https://www.sciencedirect.com/science/article/pii/S0016706114000500. Accessed: 7/10/2019.

Nelson, D.W. & Sommers, L.E. 1996. Total carbon, organic carbon, and organic matter. In: *Methods of Soil Analysis: Part 3 Chemical Methods* (eds. Sparks, D., Page, A. & Helmke, P.), pp. 961–1010. 5th ed. Soil Science Society of America.

Ngosong, C., Gabriel, E., & Ruess, L. (2012). Use of the signature fatty acid 16:1 ω 5 as a tool to determine the distribution of Arbuscular Mycorrhizal fungi in soil. *Journal of Lipids*, *2012*, 1–8.

Ngosong, C., Jarosch, M., Raupp, J., Neumann, E., & Ruess, L. (2010). The impact of farming practice on soil microorganisms and arbuscular mycorrhizal fungi: Crop type versus long-term mineral and organic fertilization. *Applied Soil Ecology*, *46*, 134–142. https://doi.org/10.1016/j.apsoil.2010.07.004

Nicolitch, O., Feucherolles, M., Churin, J. L., Fauchery, L., Turpault, M. P., & Uroz, S. (2019). A microcosm approach highlights the response of soil mineral weathering bacterial communities to an increase of K and mg availability. *Scientific Reports*, *9*, 1–13. www.nature.com/scientificreports. Accessed: 15/7/2020.

Ninyerola, M., Pons, X., & Roure, J. M. (2000). A methodological approach of climatological modelling of air temperature and precipitation through GIS techniques. *International Journal of Climatology*, *20*, 1823–1841.

Nouri, E., Breuillin-Sessoms, F., Feller, U. & Reinhardt, D. 2014. Phosphorus and nitrogen regulate arbuscular mycorrhizal symbiosis in petunia hybrida (BE Dutilh, Ed. *PLoS One*, *9*, e90841, https://doi.org/10.1371/journal.pone.0090841. Accessed: 25/7/2020

Oh, S. Y., & Lim, Y. W. (2018). Root-associated bacteria influencing mycelial growth of Tricholoma matsutake (pine mushroom). *Journal of Microbiology*, *56*, 399–407. https://doi.org/10.1007/s12275-018-7491-y. Accessed: 19/9/2019.

Olsson, P. A. (1999). Signature fatty acids provide tools for determination of the distribution and interactions of mycorrhizal fungi in soil. *FEMS Microbiology Ecology*, *29*, 303–310.

Olsen, S. R., Cole, C., & Dean, L. A. (1954). *Estimation of available phosphorus in soils by extraction with sodium bicarbonate* (1–19). USA: US Department of Agriculture.

Orwin, K. H., Dickie, I. A., Holdaway, R., & Wood, J. R. (2018). A comparison of the ability of PLFA and 16S rRNA gene metabarcoding to resolve soil community change and predict ecosystem functions. *Soil Biology and Biochemistry*, *117*, 27–35. https://doi.org/10.1016/j.soilbio.2017.10.036

Oudemans, P. V., Polashock, J. J., & Vinyard, B. T. (2008). Fairy ring disease of cranberry: Assessment of crop losses and impact on cultivar genotype. *Plant Disease*, *92*, 616–622. http://www.state.nj.us/dep/gis/newgps.htm. Accessed: 29/1/2020.

Peng, W., Zhu, Y., Song, M., Du, H., Song, T., Zeng, F., Zhang, F., Wang, K., Luo, Y., Lan, X., & Zhang, J. (2019). The spatial distribution and drivers of soil microbial richness and diversity in a karst broadleaf forest. *Forest Ecology and Management*, *449*, 1–8.

Ramesh, G., Vedha Hari, B. N., & Dhevendaran, K. (2012). Microbial association with selected medicinal plants in rhizosphere and their biodiversity. *Advances in Natural and Applied Science*, *6*, 947–958.

R Core Team (2020). R: A Language and Environment for Statistical Computing.

Richter, A., Schöning, I., Kahl, T., Bauhus, J., & Ruess, L. (2018). Regional environmental conditions shape microbial community structure stronger than local forest management intensity. *Forest Ecology and Management*, *409*, 250–259. https://www.sciencedirect.com/science/article/pii/S0378112717314202. Accessed: 19/2/2019.

Ripley, B., Hornink, K., Gebhardt, A. & Firth, D. (2018). Package 'MASS'. Accessed: 18/3/2019.

Santos, I. C., Chaumette, A., Smuts, J., Hildenbrand, Z. L., & Schug, K. A. (2019). Analysis of bacteria stress responses to contaminants derived from shale energy extraction. *Environmental Science: Processes and Impacts*, *21*, 269–278.

Sardans, J., & Peñuelas, J. (2015). Potassium: A neglected nutrient in global change. *Global Ecology and Biogeography*, *24*, 261–275. https://doi.org/10.1111/geb.12259. Accessed: 15/7/2020.

Shantz, H. L., & Piemeisel, R. L. (1917). Fungus fairy rings in eastern Colorado and their effect on vegetation. *Journal of Agriculture Research*, *11*, 191–245. https://naldc.nal.usda.gov/download/IND43965929/PDF. Accessed: 19/9/2019.

Sheldon, N. D. (2018). Using carbon isotope equilibrium to screen Pedogenic carbonate oxygen isotopes: Implications for Paleoaltimetry and Paleotectonic studies. *Geofluids*, *2018*, 1–11.

Siddikee, M. A., Zereen, M. I., Li, C. F., & Dai, C. C. (2016). Endophytic fungus Phomopsis liquidambari and different doses of N-fertilizer alter microbial community structure and function in rhizosphere of rice. *Scientific Reports*, *6*, 32270. http://www.nature.com/articles/srep32270. Accessed: 7/10/2019.

Simard, R. R. (1993). Ammonium acetate-extractable elements. In *Soil sampling and methods of analysis* (pp. 39–42). Lewis Publisher FL.

Stevenson, B. A., Kelly, E. F., McDonald, E. V., & Busacca, A. J. (2005). The stable carbon isotope composition of soil organic carbon and pedogenic carbonates along a bioclimatic gradient in the Palouse region, Washington state, USA. *Geoderma*, *124*, 37–47.

Taylor, M. D. (2000). Determination of total phosphorus in soil using simple Kjeldahl digestion. *Communications in Soil Science and Plant Analysis*, *31*, 2665–2670. https://doi.org/10.1080/00103620009370616. Accessed: 7/9/2020.

ter Braak, C. J. F., & Šmilauer, P. (2018). *Canoco reference manual and user's guide: software for ordination, version 5.10* (p. 536). Ithaca USA: Microcomputer Power.

Wang, Z., Yang, S., Wang, R., Xu, Z., Feng, K., Feng, X., Li, T., Liu, H., Ma, R., Li, H., & Jiang, Y. (2020). Compositional and functional responses of soil microbial communities to long-term nitrogen and phosphorus addition in a calcareous grassland. *Pedobiologia*, *78*, 150612.

Yang, C., Li, J., Liu, N., & Zhang, Y. (2019). Effects of fairy ring fungi on plants and soil in the alpine and temperate grasslands of China. *Plant and Soil*, *441*, 499–510. https://doi.org/10.1007/s11104-019-04141-7. Accessed: 19/9/2019.

Yang, C., Li, J., Zhang, F., Liu, N., & Zhang, Y. (2018). The optimal Redfield N: P ratio caused by fairy ring fungi stimulates plant productivity in the temperate steppe of China. *Fungal Ecology*, *34*, 91–98. https://www.sciencedirect.com/science/article/pii/S1754504818301831. Accessed: 19/9/2019.

Yang, C., Zhang, F., Liu, N., Hu, J., & Zhang, Y. (2018). Changes in soil bacterial communities in response to the fairy ring fungus Agaricus gennadii in the temperate steppes of China. *Pedobiologia*, *69*, 34–40. https://www.sciencedirect.com/science/article/pii/S0031405617302330. Accessed: 19/9/2019.

Zelles, L. (1999). Fatty acid patterns of phospholipids and lipopolysaccharides in the characterisation of microbial communities in soil: A review. *Biology and Fertility of Soils*, *29*, 111–129. https://doi.org/10.1007/s003740050533. Accessed: 18/3/2019.

Zhang, J., Ekblad, A., Sigurdsson, B. D., & Wallander, H. (2020). The influence of soil warming on organic carbon sequestration of arbuscular mycorrhizal fungi in a sub-arctic grassland. *Soil Biology and Biochemistry*, *147*, 107826.

Zotti, M., Bonanomi, G., Mancinelli, G., Barquero, M., De Filippis, F., Giannino, F., Mazzoleni, S., & González-Andrés, F. (2021). Riding the wave: Response of bacterial and fungal microbiota associated with the spread of the fairy ring fungus Calocybe gambosa. *Applied Soil Ecology*, *163*, 103963.

Zotti, M., De Filippis, F., Cesarano, G., Ercolini, D., Tesei, G., Allegrezza, M., Giannino, F., Mazzoleni, S., & Bonanomi, G. (2020). One ring to rule them all: An ecosystem engineer fungus fosters plant and microbial diversity in a Mediterranean grassland. *New Phytologist*, *227*, 884–898. https://www.researchgate.net/publication/340513485. Accessed: 10/6/2020.

SUPPORTING INFORMATION

Additional supporting information may be found in the online version of the article at the publisher's website.

How to cite this article: Rodríguez, A., Ibáñez, M., Bol, R., Brüggemann, N., Lobo, A., Jimenez, J. J., Ruess, L., & Sebastià, M.-T. (2022). Fairy ring-induced soil potassium depletion gradients reshape microbial community composition in a montane grassland. *European Journal of Soil Science*, *73*(3), e13239. https://doi.org/10.1111/ejss.13239